Simulation of polarization-insensitive multiple-quantum-well superluminescent diodes

Han Zhao (赵 涵), Yidong Huang (黄翊东), Wei Zhang (张 巍), and Jiangde Peng (彭江得)

Department of Electronic Engineering, Tsinghua University, Beijing 100084

Received July 12, 2005

The 1.3-μm polarization-insensitive superluminescent diodes (SLDs) with weak tensile strained multiple-quantum-well (MQW) and complex strained MQW were demonstrated theoretically based on the simulation of energy band structure and gain spectra at different injected carrier densities. Compared with the weak tensile strained MQW, the complex strained MQW gets higher modal gain and better modal gain matching between TE and TM modes, and the polarization sensitivity of TE and TM optical spectra can remain less than 1.0 dB over a bandwidth of 200 nm.

OCIS codes: 230.0230, 230.3670, 230.0250.

Superluminescent diodes (SLDs) are the optimum light sources in optical fiber gyroscopes and optical time domain reflectrometry (OTDR) applications because of their low coherence and relative high output power[1−4]. However, the optical output powers of common SLDs differ greatly between the TE and TM modes, which restricts their performances in highly sensitive fiber gyroscopes and optical sensors, and makes polarization-maintained optical fibers and other polarization-control optical devices have to be equipped in these applications[5]. To get polarization-insensitive SLDs, the modal gain of TE and TM modes should be designed to be similar. In common compressively strained multiple-quantum-well (MQW) SLDs, the optical gain is much larger for the TE mode than for the TM mode. Introducing tensile strain into active layers offers a promising way to enhance TM mode gain and thus to achieve polarization-insensitive output power[5−8]. Using this method, matched modal gain between TE and TM modes only at a single wavelength have been reported[5,8]. However, to match TE and TM mode gains within a wide wavelength band, which is more significant for polarization-insensitivity SLD, is more difficult because the different carrier recombination rates make the TE and TM mode gain spectra be quite different. In this paper, aiming at matching modal gain between TE and TM modes within a wide wavelength band, we propose two methods to attain the polarization insensitivity. One is using weak tensile strained quantum-well (QW), and the other is using the complex strained MQW, which is the combination of tensile strained and compressively strained MQW.

Our simulation was based on the multi-sub-band effective mass method ($\mathbf{k}\cdot\mathbf{p}$ method). To take into account the valence sub-band mixture between heavy-hole (HH) and light-hole (LH) sub-bands, 4×4 Luttinger-Kohn Hamiltonian[9] was considered. The influence of strain was simulated by introducing the strain Hamiltonian[10,11]. For the conduction band, a simple parabolic band model was used. By calculating the fine structure in the valence bands considering the band mixing effects and strain influences, gain spectra for TE and TM modes were calculated respectively at different injected carrier densities.

Under tensile strain, the energy level of the LH sub-band rises up, as shown in Fig. 1, which increases the recombination rate between the conduction and the LH sub-bands and enhances the TM mode gain. There are two main approaches of employing tensile strain to get the same TE and TM mode gains. One is introducing proper weak tensile strain into a single QW to let the TE mode gain equal to the TM mode gain. MQW consisting of several such weak tensile strained QWs can get higher balanced gains between TE and TM modes. The other is using complex strained MQW, which is the combination of tensile strained and compressively strained MQW. The tensile strained QW mainly contributes to the TM mode gain whereas the compressively strained QW to the TE mode gain. The total balanced modal gain is controlled both by choosing a suitable amount of compressive and tensile strains in the MQW active region and by suitably combining the well number of compressively strained QWs with that of the tensile strained QWs. Through careful calculation, we got two MQW structures for 1.3-μm polarization-insensitive InGaAsP/InGaAsP/InP SLDs, where TE and TM mode gains got balance in a wide wavelength band. The band structures are plotted in Fig. 2. Figure 2(a) is the weak tensile strained (−0.036%) MQW with 10-nm width and 1.3-μm central wavelength and Fig. 2(b) is the complex strained MQW, three 5-nm compressively strained wells and two 8-nm tensile strained wells are used, the strains are +0.89% and −0.96%, respectively. The barriers of these two structures are lattice-matched to InP substrate.

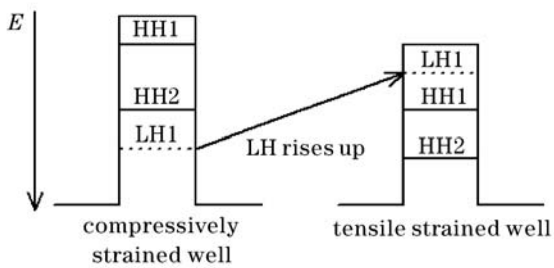

Fig. 1. Confined states of the HH and LH sub-bands in compressively strained and tensile strained QWs.

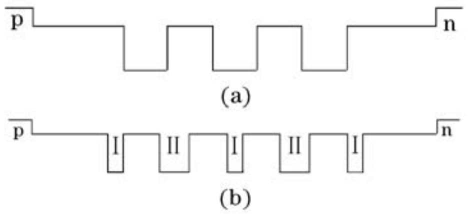

Fig. 2. Band structures of the active regions for −0.036% weak tensile strained InGaAsP MQW with 10-nm width and 1.3-μm central wavelength (a) and complex strained InGaAsP MQW with three 5-nm-wide, +0.89% compressively strained wells (I) and two 8-nm-wide, −0.96% tensile strained wells (II). The central wavelength is fixed at 1.3 μm. The InGaAsP barriers of both structures ($\lambda_g = 1.08$ μm) are lattice-matched to InP substrate.

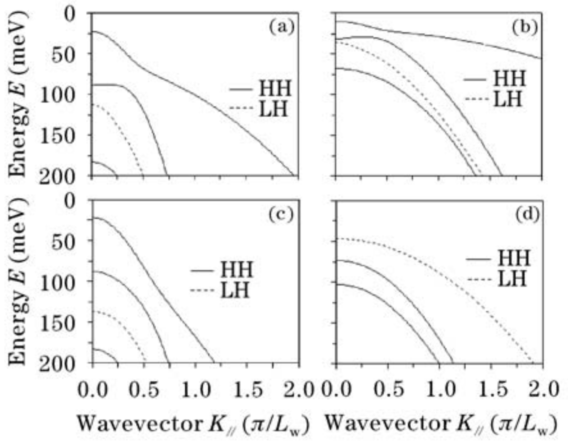

Fig. 3. Valence sub-band structures of InGaAsP QW grown on InGaAsP barrier ($\lambda_g = 1.08$ μm) lattice-matched to InP substrate for 5-nm-wide, +0.7% compressively strained QW (a), 10-nm-wide, −0.036% tensile strained QW (b), 5-nm-wide, +0.89% compressively strained QW (c), and 8-nm-wide, −0.96% tensile strained QW (d). The central wavelength of QW is fixed at 1.3 μm.

Figure 3 shows the valence sub-band structures of the different wells in Fig. 2. Figure 3(a) shows the common QW with +0.7% compressive strain for comparison with those of proposed MQW structures, Fig. 3(b) is the valence sub-band structure of weak tensile strained QW (Fig. 2(a)), Fig. 3(c) is the valence sub-band structure of compressively strained QW and 3(d) is that of tensile strained QW, Figs. 3(c) and (d) constitute the complex strained MQW (Fig. 2(b)). Introducing different strains can vary sub-band mixing effect, thus changing the sub-band shape and the gain characteristics. Compared with common sub-band structure in Fig. 3(a), the LH sub-band rises up properly in Fig. 3(b) under weak tensile strain, which enhances the transition between the conduction and LH sub-bands, thus the TE and TM mode gains can get balanced. In Fig. 3(c), LH sub-band moves downwards obviously thus TE mode gain exceeds TM mode gain greatly, whereas in Fig. 3(d), LH sub-band moves upwards obviously thus TM mode gain is much larger than TE mode gain. Therefore, the proper combination of Figs. 3(c) and (d) is expected to realize the matching between TE and TM mode gains and corresponding polarization-insensitive SLDs.

Based on the sub-band structures, we calculated gain spectra of TE and TM modes and plotted the results in Fig. 4. The influence of optical confinement factor was considered because the well widths of the two types of MQWs in our simulation were different. We are concerned more about the gain in higher carrier concentration (about 5×10^{18} cm^{-3}) in SLDs because the carrier density is not fixed at the threshold level as common laser diodes (LDs). From the gain spectra, we can see that the TE and TM mode gain spectra match well around 1.3 μm in both weak tensile strained MQW and complex strained MQW. The latter matches better than the former, the reason is that in the complex strained MQW, we can adjust the TE and TM mode gains respectively to make a perfect matching. When the carrier density is 5×10^{18} cm^{-3}, the maximum mode gain is more than 100 cm^{-1} in complex strained MQW, which is adequate to attain the output power of 50—100 mW in theory[12,13]. Moreover, TE and TM modes have nearly the same modal gain spectra in a wavelength band of 220 nm. Through calculation[14], we expected that the polarization sensitivity remains less than 1.0 dB over a bandwidth of 200 nm, which is much larger than 90 nm reported in Ref. [8].

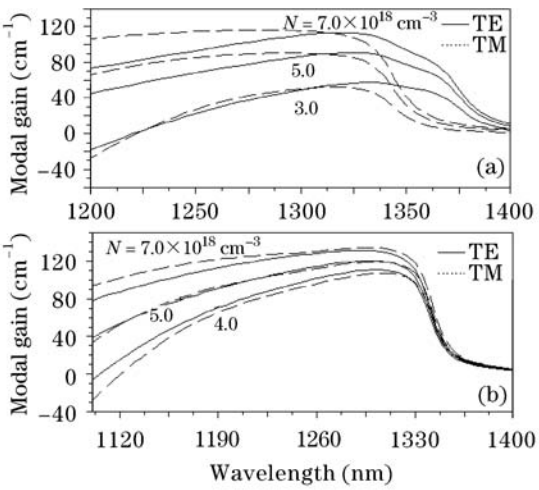

Fig. 4. Modal gain spectra of TE and TM modes for weak tensile strained MQW at injected carrier density of 3.0×10^{18}, 5.0×10^{18}, 7.0×10^{18} cm^{-3} (a) and complex strained MQW at injected carrier density of 4.0×10^{18}, 5.0×10^{18}, 7.0×10^{18} cm^{-3} (b).

Figure 5 shows the calculated peak modal gains as functions of the injected sheet carrier density for comparing the gain performances in weak tensile strained MQW and complex strained MQW with different thicknesses. From the results we can see that the complex strained MQW gets higher gain than the weak tensile strained MQW at the same sheet carrier density. This is because we get both TE and TM mode gains in a single QW in weak tensile strained MQW, there is a trade off between getting high gain and attaining TE and TM mode gain balance. While in complex strained MQW, each QW contributes to either TE or TM mode gain, so we can optimize the design of compressively strained and tensile strained QWs respectively to get both high TE and high TM mode gains. However, the advantage of weak tensile strained MQW is that its epitaxial layer growth is easier than the complex strained MQW.

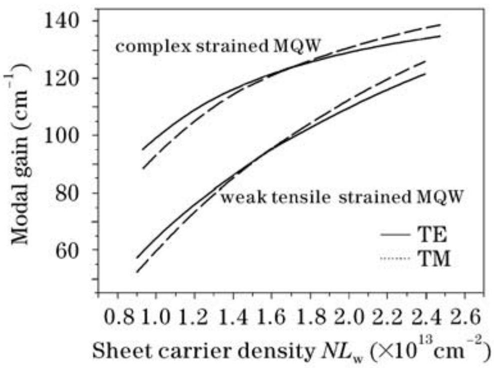

Fig. 5. Modal gains of TE and TM modes at peak gain wavelength in weak tensile strained MQW and complex strained MQW versus the injected sheet carrier density $NL_{\rm w}$, where N is the injection carrier density and $L_{\rm w}$ is the total well thickness.

In conclusion, based on the calculated energy band structure under proper strain, the gain spectra of weak tensile strained MQW and complex strained MQW were simulated for realizing polarization-insensitive SLDs. We carefully calculated the parameters in both types of MQWs and obtained well matched TE and TM mode output spectra in a wide wavelength band around 1.3 μm. The complex strained MQW gets higher modal gain and better matching between TE and TM modes than tensile strained MQW, and the polarization sensitivity can remain less than 1.0 dB over a bandwidth of 200 nm with complex strained MQW.

H. Zhao's e-mail address is zhaohan00@mails.tsinghua.edu.cn, and Y. Huang's e-mail address is yidonghuang@mail.tsinghua.edu.cn.

References

1. N. S. K. Kwong, K. Y. Lau, and N. Bar-Chaim, IEEE J. Quantum Electron. **25,** 696 (1989).
2. B. D. Patterson, J. E. Epler, B. Graf, H. W. Lehmann, and H. C. Sigg, IEEE J. Quantum Electron. **30,** 703 (1994).
3. J. H. Song, S. H. Cho, I. K. Han, Y. Hu, P. J. S. Heim, F. G. Johnson, D. R. Stone, and M. Dagenais, IEEE Photon. Technol. Lett. **12,** 783 (2000).
4. S. Wang, H. Zhu, Z. Liu, R. Zhang, Y. Ding, L. Zhao, F. Zhou, J. Bian, L. Wang, and W. Wang, Chin. Opt. Lett. **2,** 359 (2004).
5. O. Mikami, Y. Noguchi, K. Magari, and Y. Suzuki, IEEE Photon. Technol. Lett. **4,** 703 (1992).
6. K. Magari, M. Okamoto, and Y. Noguchi, IEEE Photon. Technol. Lett. **3,** 998 (1991).
7. M. Silver, A. F. Phillips, A. R. Adams, P. D. Greene, and A. J. Collar, IEEE J. Quantum Electron. **36,** 118 (2000).
8. H. Ma, S. Chen, X. Yi, G. X. Zhu, and J. Jin, Opt. Quantum Electron. **36,** 551 (2004).
9. J. M. Luttinger and W. Kohn, Phys. Rev. **97,** 869 (1955).
10. A. Twardowski and C. Hermann, Phys. Rev. B **35,** 8144 (1987).
11. D. Ahn and S.-L. Chuang, IEEE J. Quantum Electron. **26,** 13 (1990).
12. G. A. Alphonse, Proc. SPIE **4648,** 125 (2002).
13. A. T. Semenov, V. R. Shidlovski, M. E. Lipin, and V. E. Rafailov, Proc. SPIE **3860,** 480 (1999).
14. V. Shidlovshi and J. Wei, Proc. SPIE **4648,** 139 (2002).